# X-ray Spectrometry

# 32



## CHAPTER PREVIEW

To use the X-rays generated when the electron beam strikes a TEM specimen, we have to detect them first and then identify them as coming from a particular element. This is accomplished by X-ray spectrometry, which is one way we can transform a TEM into a far more powerful instrument, called an analytical electron microscope (AEM). Currently, the only kind of X-ray spectrometer that we use in an AEM is an X-ray energy-dispersive spectrometer (XEDS), which comprises a detector interfaced to signal-processing electronics and a computer-controlled multichannel analyzer (MCA) display. The XEDS is a complex and rather sophisticated piece of instrumentation which takes advantage of modern semiconductor technology. The principal component of the XEDS is a semiconductor detector which has the benefit of being compact enough to fit within the confined region of the TEM stage and, in one form or another, is sensitive enough to detect all the elements above Li in the periodic table.

We start with the basic physics you need to understand how the detector works and give you a very brief overview of the processing electronics. We then describe a few simple tests you can perform to confirm that your XEDS is working correctly. It is really most important from a practical point of view that you know the limitations of your XEDS system. Therefore, we will describe these limitations in some detail, especially the unavoidable artifacts. Finally, we briefly mention the wavelength-dispersive spectrometer (WDS), which is used in bulk X-ray microanalysis. The WDS is old technology which might see a renaissance in the AEM in the future.



D. B. Williams et al., *Transmission Electron Microscopy*

# X-ray Spectrometry

# 32

## 32.1. X-RAY ANALYSIS: WHY BOTHER?

When characterizing a specimen in the TEM, the limitations of only using imaging should by now be obvious to you. Our eyes are accustomed to the interpretation of 3D reflected-light images. However, as we have seen in great detail in Part III, the TEM gives us two-dimensional projected images of 3D transparent specimens and you, the operator, need substantial experience in order to interpret the images correctly. For example, Figure 32.1 shows six images, taken with both light and electron microscopes (can you distinguish which images are from which kind of microscope?). The scale of the microstructures varies from nanometers to millimeters and yet the images appear very similar. Without any prior knowledge it would be almost impossible, even for an experienced microscopist, to identify the nature of these specimens simply by looking at the image.

Now if you look at Figure 32.2, you can see six X-ray spectra, one from each of the specimens in Figure 32.1. We will be discussing such spectra in detail later in this and subsequent chapters, but even with no knowledge of XEDS, you can easily see that each specimen gives a different spectrum.

> Different spectra mean that each specimen must have a different elemental composition and it is possible to obtain this information in a matter of minutes.

Armed with the elemental make-up of your specimen, any subsequent image and diffraction analysis is greatly facilitated. For your interest, the identity of each specimen is given in the caption to Figure 32.2. While Figures 32.2A–E are all from common inorganic materials, Figure 32.2F is from a cauliflower which, once you get it into the electron microscope, provides a very distinctive spectrum. The familiar morphology of this specimen, now obvious in Figure 32.1F, also accounts for the generic term "cauliflower structure" which is given to these and other similar microstructures.

> The main message you should get from this illustration is that the *combination* of imaging and spectrometry is most powerful and this combination transforms a TEM to an AEM.

Within a very short time, you can get a qualitative elemental analysis of most features in a complex microstructure, and the important features can be isolated for full quantitative analysis, which we will address in Chapter 35. In the chapters before this you will first learn something about how the XEDS detector works and the problems that arise when the detector is inserted into the column of an AEM.

## 32.2. BASIC OPERATIONAL MODE

To produce spectra such as those in Figure 32.2, all that you have to do is obtain a TEM or STEM image of the area you wish to analyze. In TEM mode, you then have to condense the beam down to an appropriate size for analysis. This may mean exciting the C1 lens more strongly and changing the C2 aperture and C2 lens strength. These steps may misalign the illumination system. For this reason it is recommended that you operate in STEM mode. Create your STEM image using the appropriate C1 lens setting and C2 aperture to give the desired probe dimension. It is then a simple matter to stop the scanning probe and position it on the feature you wish to analyze. Furthermore, critical software routines that you can use to check for specimen drift during your analysis can only work via a digital image of the analysis region.

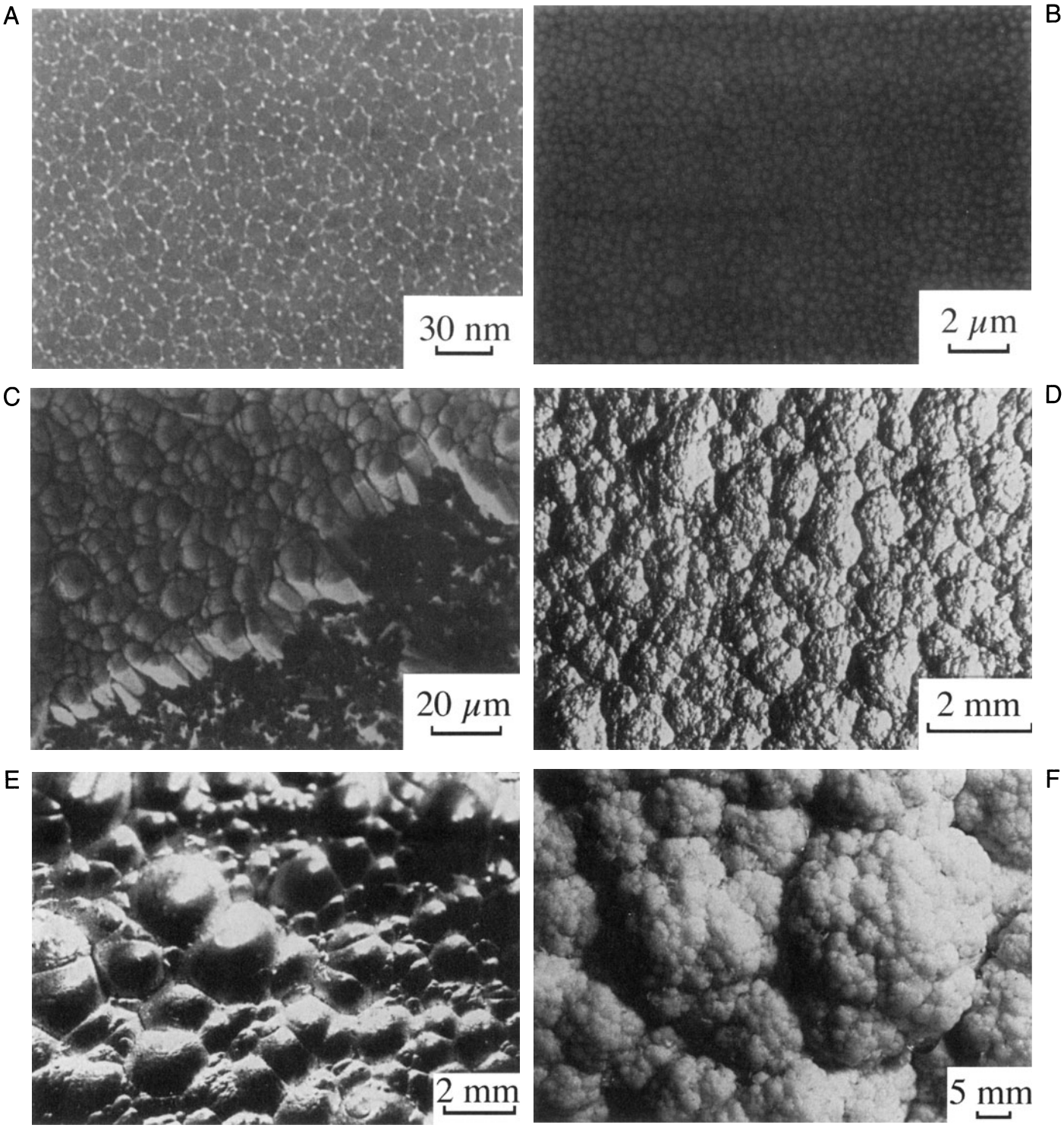


**Figure 32.1.** Six images of various microstructures, spanning the dimensional range from nanometers to millimeters. The images were taken with TEMs, SEMs, and light microscopes, but the characteristic structures are very similar, and it is not possible, without prior knowledge, to identify the samples.

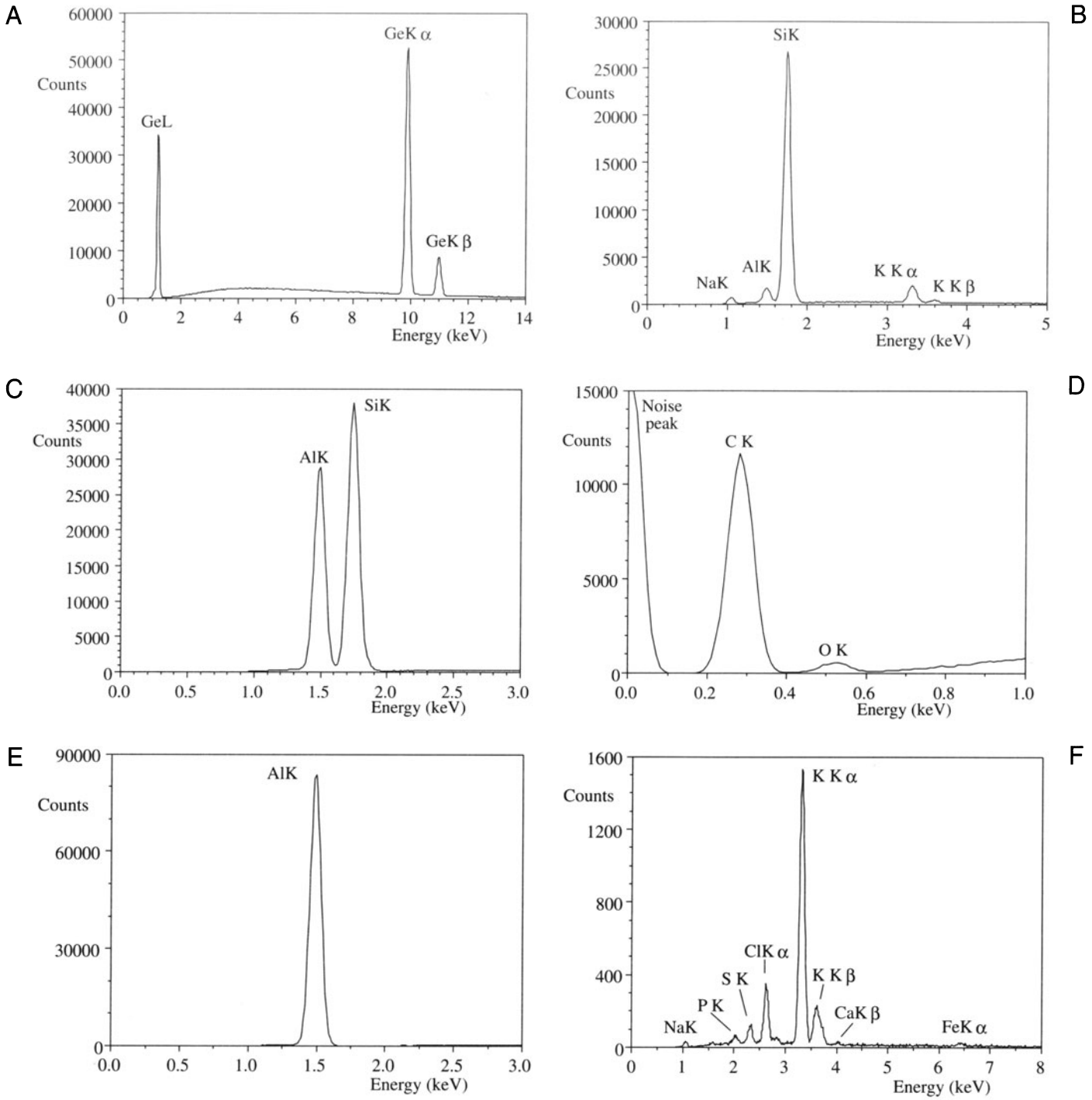


**Figure 32.2.** XEDS spectra from the six materials in Figure 32.1. Each spectrum is clearly different from the others, and helps to identify the samples as (A) pure Ge, (B) silica glass, (C) Al evaporated on a Si substrate, (D) pyrolitic graphite, (E) pure Al, and (F) a cauliflower.

Use STEM images to select your analysis region. This makes it easier to move between image mode and analysis mode.

Microanalysis should *always* be performed with your specimen in a low-background (Be) holder (see Chapter 8). The holder should be capable of being cooled to liquid-$N_2$ temperature to minimize contamination, and a double-tilt version is recommended so diffraction and imaging can be carried out simultaneously.

## 32.3. THE ENERGY-DISPERSIVE SPECTROMETER

The XEDS produces spectra which are plots of X-ray *counts* (imprecisely termed "intensity") versus X-ray *energy*. Before we get into details, recall from back in Chapter 4 that electrons generate two kinds of X-rays. When electrons ionize an atom, the emitted characteristic X-ray *energy* is unique to the ionized atom. When electrons are slowed by interaction with the nucleus, they produce a continuum of bremsstrahlung X-rays. The result is that, as we have seen in Figures 1.4A, 4.6, and 32.2, the characteristic X-rays appear as Gaussian-shaped peaks superimposed on a background of bremsstrahlung X-rays, most clearly visible in Figure 32.2A. Many more spectra will appear throughout this and subsequent chapters.

The XEDS was developed in the late 1960s and, by the mid-1970s, it was available as an option on many TEMs and even more widespread on other electron beam instruments, such as SEMs. This testifies to the fact that the XEDS is really quite a remarkable instrument, embodying many of the most advanced features of semiconductor technology. It is compact, stable, robust, easy to use, and you can quickly interpret the readout. Several books have been devoted to XEDS and these are listed in the general reference section. Figure 32.3A shows a schematic diagram of an XEDS system and we'll deal with each of the major components as we go through this chapter.

The three main parts are the detector, the processing electronics, and the MCA display.

A computer controls all three parts. First, it controls whether the detector is on or off. Ideally, we only want to process one incoming X-ray at a time so the detector is switched off when an X-ray signal is detected. Second, the computer controls the processing electronics, setting the time required to analyze the X-ray signal and assigning

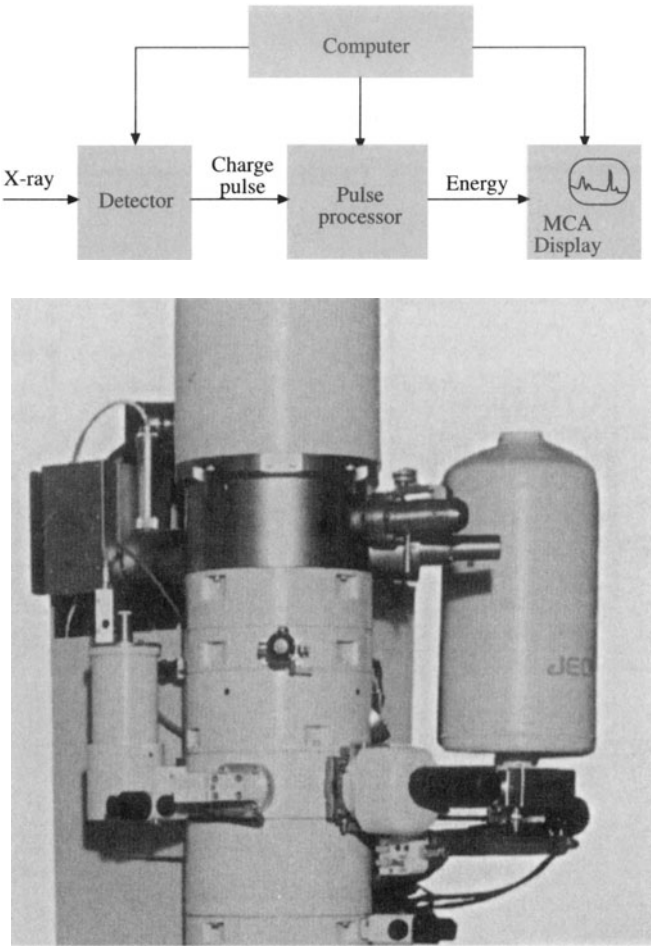


**Figure 32.3.** (A) Diagram of the XEDS system showing how the computer controls the detector, the processing electronics, and the display. (B) An XEDS system interfaced to the stage of an AEM. All that is visible is the large liquid-$N_2$ dewar attached to the side of the column.

the signal to the correct channel in the MCA. Third, the computer software governs both the calibration of the spectrum readout on the MCA screen and all the alphanumerics which tell you the conditions under which you acquired the spectrum. Any data processing is also carried out using the computer.

We can summarize the working of the XEDS as follows:

- The detector generates a charge pulse proportional to the X-ray energy.
- This pulse is first converted to a voltage.
- Then the signal is amplified through a field effect transistor (FET), isolated from other pulses, further amplified, then identified elec-

tronically as resulting from an X-ray of specific energy.
- Finally, a digitized signal is stored in a channel assigned to that energy in the MCA.

The speed of this process is such that the spectrum appears to be generated in parallel with the full range of X-ray energies detected simultaneously, but the process actually involves very rapid serial processing of individual X-ray signals. Thus the XEDS both detects X-rays and separates (disperses) them into a spectrum according to their *energy*, hence the name of the spectrometer.

Figure 32.3B shows a detector interfaced to an AEM. In fact, you can't see the processing electronics or the MCA display, nor the detector itself because it sits close to the specimen within the microscope column. The most prominent feature that you can see is the liquid-$N_2$ dewar, which cools the detector.

## 32.4. SEMICONDUCTOR DETECTORS

The detector in an XEDS is a reverse-biased p-i-n diode. Almost all AEMs use silicon–lithium [Si(Li)] semiconductor detectors and so we will take these as our model. Later, in Section 32.4.C, we'll discuss the role of intrinsic Ge (IG) detectors, which can be useful on intermediate voltage AEMs.

### 32.4.A. How Does XEDS Work?

While you don't need to understand precisely how the detector works in order to use it, a basic understanding will help you optimize your system and it will also become obvious why certain experimental procedures and precautions are necessary.

When X-rays interact with a semiconductor, the primary method of energy deposition is the transfer of electrons from the valence band to the conduction band, creating an electron–hole pair. High-energy electrons lose energy in Si in a similar way as we saw in Section 4.4. The energy required for this transfer in Si is ~3.8 eV at the liquid-$N_2$ operating temperature. (This quantity is a statistical value so don't try to link it directly to the band gap.) Since characteristic X-rays typically have energies well in excess of 1 keV, thousands of electron–hole pairs can be generated by a single X-ray. The number of electrons or holes created is directly proportional to the energy of the incoming X-ray. Even though all the X-ray energy is not, in fact, converted to electron–hole pairs, enough are created for us to collect sufficient signal to distinguish most elements in the periodic table with good statistical precision. The way this is achieved is summarized in Figure 32.4, which is a schematic diagram of the Si(Li) detector.

The design of the Si(Li) detector is very similar to the semiconductor electron detectors discussed in Chapter 7.

> The electron detectors separate the electrons and holes by the internal reverse bias of a very narrow p-n junction; since X-rays penetrate matter much more easily than electrons, we need a much thicker region for the X-rays to generate electron–hole pairs and lose all their energy.

In practice, we need to have an intrinsic region between p- and n-type regions which is about 3 mm thick. So the Si should have low conductivity, with no impurity atoms to contribute electrons or holes to the charge pulse, and no defects to act as recombination sites for the electron–hole pairs. However, we still cannot make intrinsic Si on a commercial basis. It usually contains acceptor impurities and so acts as a p-type semiconductor. We compensate for the impurity effects by "filling" any recombination sites with Li, thus creating a region of intrinsic Si, hence the term Si(Li), popularly pronounced "silly." Without the Li, commercial-purity Si would suffer electrical breakdown when the bias was applied to separate the electrons and holes. The Li is introduced either by diffusion under an applied voltage (hence the term "Li-drifted" detector) or, in a more controlled fashion, by ion implantation followed by a diffusion anneal.

While many electrons and holes are generated by an X-ray, they still constitute a very small charge pulse (about $10^{-16}$ C), and so a negative bias of ~0.5–1 keV is ap-

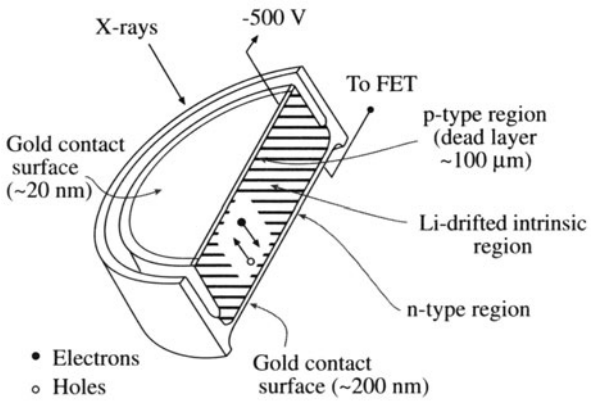


**Figure 32.4.** Cross section of a Si(Li) detector. The incoming X-rays generate electron–hole pairs in the intrinsic Si which are separated by an applied bias. A positive bias attracts the electrons to the rear ohmic contact after which the signal is amplified by an FET.

plied across the Si to ensure collection of most of the signal. We apply the bias between ohmic contacts, which are evaporated metal films such as Au or Ni, ~10–20 nm thick for the front face and ~200 nm at the back. This metal film also produces a p-type region at the front of the crystal; the back of the crystal is doped to produce n-type Si.

So the whole crystal is now a p-i-n device, with relatively shallow junctions less than 200 nm deep at either side of the central 3-mm intrinsic region.

When a reverse bias is applied to the crystal (i.e., a negative charge is placed on the p-type region at the front of the detector and a positive charge on the rear), the electrons and holes are separated and a charge pulse of electrons can be measured at the rear ohmic contact. Remember that the magnitude of this pulse is proportional to the energy of the X-ray that generated the electron–hole pairs. (We could equally well measure the whole pulse, but available low-noise FETs are n-channel devices, requiring electron collection.)

The p and n regions, at either end of the detector, are usually termed "dead layers." The traditional argument for use of this term is that the Li compensation is not completely effective so most of the electron–hole pairs generated in these end regions recombine, and contribute nothing to the charge pulse. Recently, however, Joy (1995) has shown that the dead layer can be explained if the diffusion length of the charge-carrying electrons exceeds the distance they travel under the drift field, in which case they are not "dead" but they will not be gathered at the surface electrode and contribute to the charge pulse. However, we'll still use the inaccurate term "dead layer" because it is so common. In practice it is the layer at the entrance surface of the detector that is most important since the X-rays must traverse it to be detected, and we will refer to this as *the* dead layer. This dead layer affects the spectrum, particularly when you are studying peaks from the low-$Z$ elements (McCarthy 1995).

The p and n regions are called "dead layers" and the intrinsic region in between is referred to as the "active layer."

Why do we have to cool the detector with liquid $N_2$? Well, if the detector were at room temperature, three highly undesirable effects would occur:

- Thermal energy would activate electron–hole pairs, giving a noise level that would swamp the X-ray signals we want to detect.
- The Li atoms would diffuse under the applied bias, destroying the intrinsic properties of the detector.
- The noise level in the FET would mask signals from low-energy X-rays.

For these reasons we cool the detector and the FET with liquid $N_2$, necessitating the characteristic dewar mentioned above (see Figure 32.3B). The FET gets to a temperature of about 140 K and the detector surface is at about 90 K.

Cooling the detector and the FET brings some undesirable consequences, which we have to accommodate. The minor irritations are that we have to regularly monitor and fill up the liquid-$N_2$ dewar. The more severe consequence of the cooling is that both hydrocarbons and ice from the microscope environment can condense on the cold detector surface, causing absorption of lower-energy X-rays. There are two obvious solutions to this problem. Either we can isolate the detector from the microscope vacuum, or we can remove hydrocarbons and water vapor from the microscope. The latter is the more desirable solution but the former is far easier. So, detectors are sealed in a prepumped tube with a "window" to allow X-rays through into the detector.

You have a choice of three different kinds of detector: those with a Be window, those with an ultrathin window, and those without a protective window.

Let's examine the pros and cons of each detector window; a good review has been given by Lund (1995).

## 32.4.B. Different Kinds of Windows

*Beryllium window detectors* use a thin sheet (nominally 7 μm) of beryllium which is transparent to most X-rays, and can withstand atmospheric pressure when the stage is vented to air. (In fact, 7 μm Be is expensive ($3M/pound!), rare, and slightly porous, so thicker sheet (> ~ 12 μm) is more commonly used.) Production of such thin Be sheet is a remarkable metallurgical achievement, but the window is still too thick to permit passage of all characteristic X-rays; any that have energy less than ~1 keV are strongly absorbed. Therefore, we cannot detect $K_\alpha$ X-rays from elements below about Na ($Z = 11$) in the periodic table. The Be window prevents microanalysis of the lighter elements such as B, C, N, and O, which are important in materials science (and also in other disciplines that use the AEM, such as the biological and geological sciences). Other factors, such as the low fluorescence yield and absorption within the specimen, make light-element X-ray microanalysis somewhat of a challenge, and EELS is often preferable.

*Ultrathin window (UTW) detectors* have windows that are less absorbent than Be; usually these are made from very thin (<100 nm) films of polymer, diamond, boron nitride, or silicon nitride, all of which are capable of withstanding atmospheric pressure while still transmitting 192-eV boron $K_\alpha$ X-rays. Early UTWs were very thin polymer membranes, such as parylene. Unfortunately, these were unable to withstand atmospheric pressure; they had to be withdrawn behind a vacuum isolation valve whenever a specimen was exchanged or the column was vented to air. Newer, composite Al/polymer UTWs or very thin diamond or BN windows, sometimes termed "atmospheric thin windows" (ATWs), are really the only sensible option. You should remember that different window materials absorb the light-element X-rays differently, so you need to know the characteristics of the window in the particular system you are using. For example, carbon-containing windows absorb N $K_\alpha$ X-rays very strongly.

*Windowless detectors* were first tried in the early 1970s, but microscope vacuums were relatively poor, resulting in rapid hydrocarbon and/or ice contamination of the detector surface. You should only use windowless detectors in a UHV AEM. Take great care to eliminate hydrocarbons from your specimen and keep the partial pressure of water vapor below ~$10^{-8}$ Pa by efficient pumping. The best performance by a windowless system is the detection of Be (110 eV) $K_\alpha$ X-rays as shown in Figure 32.5, which is a remarkable feat of electronics technology.

You may recall that it takes ~3.8 eV to generate an electron–hole pair in Si, so a Be $K_\alpha$ X-ray will create at most 29 electron–hole pairs, giving a charge pulse of ~$5 \times 10^{-18}$ C !

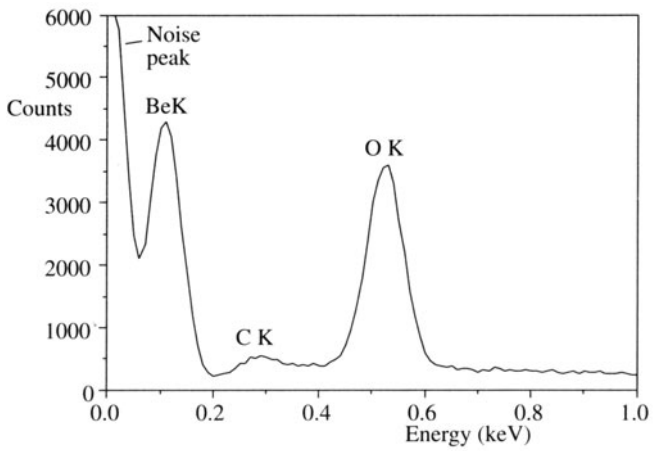


**Figure 32.5.** XEDS spectrum showing the detection of Be in an oxidized Be foil in an SEM at 10 keV. The Be $K_\alpha$ line is not quite resolved from the noise peak.

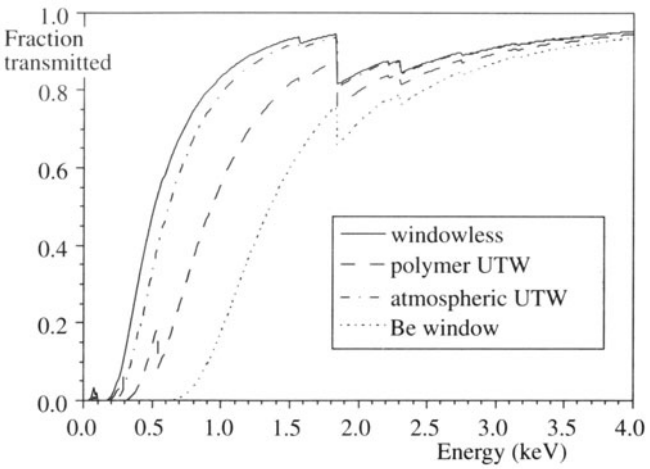


**Figure 32.6.** Low-energy efficiency calculated for a windowless detector, UTW detector (1 μm Mylar coated with 20 nm of Al), an ATW detector and a 13-μm Be window detector. Note that the efficiency is measured in terms of the fraction of X-rays transmitted by the window.

The relative performance of the various types of Si(Li) detector windows is summarized in Figure 32.6. Here we plot the detector efficiency as a function of the energy of the incoming X-ray. You can clearly see the rapid drop in efficiency at the low-energy end and the increased efficiency of UTW and windowless detectors. In fact, the Si(Li) detector absorbs X-rays with almost 100% efficiency over the energy range from about 2 to 20 keV, as shown in Figure 32.7. Within this energy range you will find X-rays from all the elements in the periodic table

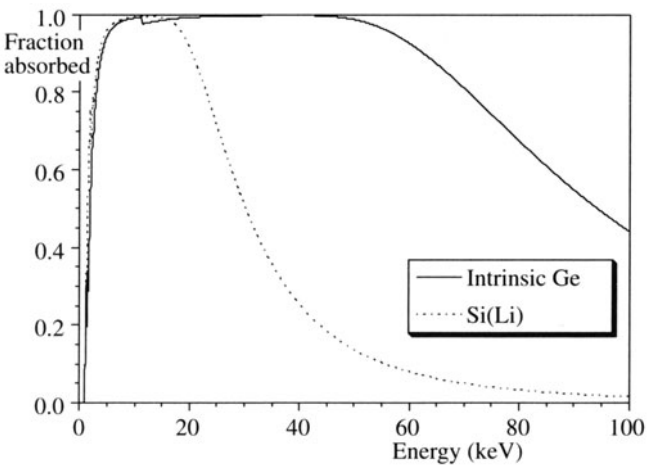


**Figure 32.7.** High-energy efficiency up to 100-keV X-ray energy calculated for Si(Li) and IG detectors, assuming a detector thickness of 3 mm in each case. Note the large effect of the Ge absorption edge at about 11 keV. In contrast to Figure 32.6, the efficiency in this case is measured by the fraction of X-rays absorbed within the detector.

above phosphorus. This uniform high efficiency is a major advantage of the XEDS detector.

## 32.4.C. Intrinsic Germanium Detectors

You can see in Figure 32.7 that Si(Li) detectors show a drop in efficiency above ~20 keV. This is because X-rays with such high energy can pass through the detector without depositing their energy by creating electron–hole pairs. This effect limits the use of Si(Li) detectors in intermediate voltage AEMs because at 300–400 keV we can generate $K_\alpha$ X-rays from all the high-atomic-number elements; Pb $K_\alpha$ X-rays at 75 keV are easily excited by 300-keV electrons. As we'll see in Chapter 35, there are certain advantages to using the K lines rather than the lower-energy L or M lines for quantification; with a Si(Li) detector the K lines from elements above silver (Z = 47) are barely detectable. The answer to this problem is to use a Ge detector, which more strongly absorbs high-energy X-rays (Sareen 1995).

We can manufacture Ge of higher purity than Si, and therefore Li compensation is not needed to produce a large intrinsic region; clearly this is a major advantage. Like the Si(Li) detector, the intrinsic Ge (IG) or high-purity Ge (HPGe) detector can have a Be window, a UTW/ATW, or no window; in any form it has some advantages over Si(Li). The detector is more robust and it can be warmed up repeatedly, which, as we'll see, sometimes solves certain problems.

> The intense doses of high-energy electrons or X-rays which can easily be generated in an AEM (e.g., when the beam hits a grid bar) can destroy the Li compensation in a Si(Li) detector, but there is no such problem in an IG crystal.

Furthermore, the intrinsic region can easily be made ~5 mm thick, which results in 100% efficient detection of Pb $K_\alpha$ X-rays at ~ 75 keV. Figure 32.7 compares the efficiency of Si(Li) and IG detectors up to 100 keV and Figure 32.8 shows detection of Pb $K_{\alpha1}$ and $K_{\alpha2}$ lines generated from a lead glass specimen at 200 kV.

There is an even more fundamental advantage to IG detectors. Since it takes only ~2.9 eV of energy to create an electron–hole pair in Ge, compared with 3.8 eV in Si, a given X-ray produces more electron–hole pairs, and so the energy resolution and signal to noise are better. However, as you may have guessed, there are some difficulties in using IG detectors. The high-energy K lines, for which these detectors are ideally suited, have very small ionization cross sections when using 300–400 keV electrons, and so the spectral intensities are rather low, as you can see in Figure 32.8. A minor drawback is that IG detectors have to be

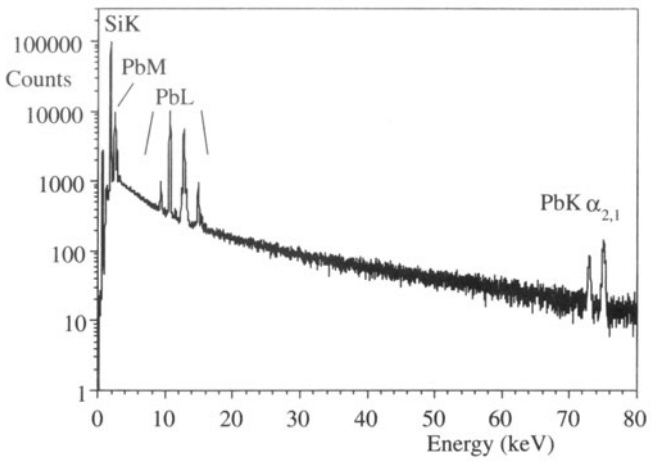


**Figure 32.8.** High-energy spectrum from lead silicate glass analyzed in a 200-kV AEM with an IG detector. Note the logarithmic scale for the counts which masks somewhat the very low intensity of the K lines compared with the L and M families. Note also that the $K_{\alpha1}$ and $K_{\alpha2}$ lines are clearly resolved.

cooled 25 K lower than Si(Li) to give the same leakage current, and they invariably need an Al-coated UTW since they are more sensitive to infrared radiation than Si(Li) detectors. This UTW reduces the maximum collection angle of IG detectors (see Section 33.2). Si(Li) detectors are easier to manufacture and are more reliable. They have a long history of dependable operation and a large number are already in use. IG detectors should eventually become more widely accepted as users install new systems.

IG detectors have been used since ~1970 by nuclear physicists to detect MeV radiation, but the first one was not installed on an AEM until 1986. One reason for this slow transfer of technology was that the high-energy K lines were very inefficiently excited in the lower voltage AEMs available at the time. Also, the low-energy performance of IG detectors was very poor in early detectors due mainly to a thick dead layer, which resulted in very non-Gaussian peak shapes. This problem has now been overcome and Gaussian characteristic peaks can be generated across the full energy range of the spectrum.

> In fact, UTW IG detectors are capable of detecting X-rays from boron to uranium, although the low-energy spectrum is still a little better in a Si(Li) system.

It is arguable that all intermediate voltage AEMs should be equipped with two detectors, an IG and a UTW Si(Li), to give the most efficient X-ray detection across the widest possible elemental range. Look ahead to Table 32.1 for a comparison of the two kinds of detector.

## 32.5. PULSE PROCESSING AND DEAD TIME

The electronic components attached to the detector convert the charge pulse created by the incoming X-ray into a voltage pulse, which can be stored in the appropriate energy channel of the MCA. The pulse-processing electronics must maintain good energy resolution across the spectrum without peak shift or distortion, even at high counting rates. To accomplish this, all the electronic components beyond the detector crystal must have low-noise characteristics and must employ some means of handling pulses that arrive in rapid succession. Currently, this whole process relies on analog pulse processing, but it is likely that, in the near future, many of the problems we'll now describe will be solved by digital techniques (Mott and Friel 1995).

Let's consider first of all what happens if a single isolated X-ray enters the detector and creates a pulse of electrons at the back of the Si(Li) crystal.

- The charge pulse enters the FET, which acts as a preamplifier and converts the charge into a voltage pulse.
- This voltage pulse is amplified several thousand times by a pulse processor, and shaped so that an analog-to-digital converter can recognize the pulse as coming from an X-ray of specific energy. (The XEDS doesn't do a very good job of accurate energy assessment.)
- The computer assigns it to the appropriate channel in the MCA display.

The accumulation of pulses or counts entering each energy channel at various rates produces a histogram of counts versus energy that is a digital representation of the X-ray spectrum. The MCA display offers multiples of 1024 channels in which to display the spectrum, and various energy ranges can be assigned to these channels. For example, 10, 20, or 40 keV full horizontal scales can be used (or even 80 keV for an IG detector on an intermediate voltage AEM). The display resolution chosen depends on the number of channels available.

A typical energy range that you might select for a Si(Li) detector is 20 keV, and in 2048 channels this gives you a display resolution of 10 eV per channel.

You should keep the display resolution at about 10 eV per channel. A smaller value ties up a lot of memory and often you can't display the whole spectrum at once. A larger value gives you only a few channels for each characteristic peak. For an IG detector, more channels (at least 4096) are needed to display the complete spectrum up to 80 or 100 keV, but the resolution of the MCA display is usually poorer, ~20 eV/channel.

Details of the pulse processing electronics are not important except for two variables over which you have control. These are the time constant and the dead time. The *time constant* ($\tau$) is the time (~10–50 μs) allowed for the pulse processor to evaluate the magnitude of the pulse. If you select a longer $\tau$, the system is better able to assign an energy to the incoming pulse, but fewer counts can be processed in a given analysis time. You have a choice of $\tau$ given by the manufacturer:

- The shortest $\tau$ (typically a few μs) will allow you to process more counts per second (cps) but with a greater error in the assignment of a specific energy to the pulse, and so the energy resolution (see Section 32.6 below) will be poorer.
- A longer $\tau$ (up to about 50 μs) will give better resolution but the count rate will be lower.

You can't have a high count rate and good resolution, so for most routine thin-foil analyses you should maximize the count rate (shortest $\tau$), unless there is a specific reason why you want to get the best possible energy resolution (longest $\tau$). This recommendation is based on a detailed argument presented by Statham (1995).

Now in reality there are many X-rays entering the detector, but because of the speed of modern electronics the system can usually discriminate between the arrival of two almost simultaneous X-rays. The details of the electronics can be found, e.g., in Goldstein *et al.* (1992). When the electronic circuitry detects the arrival of a pulse, it takes less than a microsecond before the detector is effectively switched off for the period of time called the *dead time* while the pulse processor analyzes that pulse. The dead time is clearly closely related to $\tau$, which is so small that you should expect your detector system to process up to 10,000 cps quite easily. The dead time will increase as more X-rays try to enter the detector, which closes down more often. The dead time can be defined in several ways. Take the ratio of the output count rate ($R_{out}$) to the input count rate ($R_{in}$), which you can usually measure. Then we can say

$$\text{Dead time in } \% = \left(1 - \frac{R_{out}}{R_{in}}\right) \times 100\% \qquad [32.1a]$$

An alternative definition is

$$\text{Dead time in \%} = \frac{(\text{clock time} - \text{live time})}{\text{live time}} \times 100\% \quad [32.1b]$$

Put another way, this equation says that if you ask the computer to collect a spectrum for a "live time" of 100 s, this means that the detector must be "live" and receiving X-rays for this amount of time. If it is actually dead for 20 s while it is processing the X-rays, then the dead time will be 20%, and it will take 120 s of "clock time" to accumulate a spectrum. As the input count rate increases, the output count rate will drop and the clock time will increase accordingly. Dead times in excess of 50–60% (or as little as 30% in old systems) mean that the detector is being swamped with X-rays and collection becomes increasingly inefficient, and it is better to turn down the beam current or move to a thinner area of the specimen to lower the count rate.

## 32.6. RESOLUTION OF THE DETECTOR

We can define the energy resolution $R$ of the detector as follows

$$R^2 = P^2 + I^2 + X^2 \quad [32.2]$$

The term $P$ is a measure of the quality of the associated electronics. It is defined as the full width at half maximum (FWHM) of a randomized electronic pulse generator. $X$ is the FWHM equivalent attributable to detector leakage current and incomplete charge collection (see below). $I$ is the intrinsic line width of the detector which is controlled by fluctuations in the numbers of electron–hole pairs created by a given X-ray and is given by

$$I = 2.35\left(F\varepsilon E\right)^{\frac{1}{2}} \quad [32.3]$$

Here, $F$ is the Fano factor of the distribution of X-ray counts from Poisson statistics, $\varepsilon$ is the energy to create an electron–hole pair in the detector, and $E$ is the energy of the X-ray line. Because of these two factors, the experimental resolution can only be defined under specific analysis conditions.

The IEEE standard for $R$ is the FWHM of the Mn $K_\alpha$ peak, generated (off the microscope) by an $Fe^{55}$ source which produces $10^3$ cps with an 8-μs pulse-processor time constant.

Rather than using radioactive $Fe^{55}$, we recommend measuring the detector resolution on the AEM column! Now, since Mn is not a common sample to have lying around, you will find it useful to keep a thin Cr-film specimen to check the resolution when the detector is on the column. An evaporated Cr film about 100 nm thick supported on a carbon film and a Cu grid is ideal. Because Cr is next to Mn in the periodic table, the resolution of the $K_\alpha$ peak will be just a few eV less than that of Mn. The Cr is also stable with a resilient thin oxide film; it doesn't degrade in the electron beam. As we'll see later, these Cr films are very useful for other calibration checks and performance criteria (Zemyan and Williams 1994).

Many XEDS computer systems have an internal software routine which measures the resolution. Alternatively, you can gather a Mn or Cr peak, and select a window encompassing the peaks from the channels on both sides of the peak that contain half the maximum counts in the central channel, as shown in Figure 32.9.

Typically, Si(Li) detectors have a resolution of ~140 eV at Mn $K_\alpha$ with the best being 127 eV. The best reported IG resolution is 114 eV.

Because the value of $\varepsilon$ is lower for Ge (2.9 eV) than for Si (3.8 eV), IG detectors have higher resolution than Si(Li). The resolution is also a function of the area of the detector, and the values given relate to the performance of 10-$mm^2$ detectors. The 30-$mm^2$ detectors which are usually installed on AEMs have resolutions about 5 eV worse than the figures just mentioned. However, you should also be aware that when $R$ is measured on the microscope, there

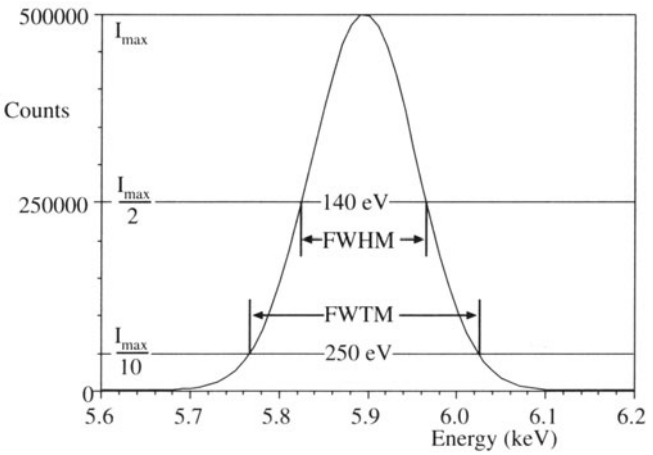


**Figure 32.9.** Measurement of the energy resolution of an XEDS detector by determining the number of channels that encompass the FWHM of the Mn $K_\alpha$ peak. The number of channels multiplied by the eV per channel gives the resolution, which typically should be about 130–140 eV. We can measure the FWTM also to give an indication of the degree of the incomplete charge collection which distorts the low-energy side of the peak. The FWTM should be ~1.82 times the FWHM.

may be a further degradation in resolution. It is rare to find a 30-mm$^2$ Si(Li) detector delivering a resolution much better than 140 eV on the AEM column, even though the quoted values are typically ~10 eV lower.

Remember also that there is always a trade-off between resolution and count rate, unless digital pulse processing is used.

How close are XEDS detectors to their theoretical resolution limit? If we assume that there is no leakage and the electronics produced no noise, then $P = X = 0$ in equation 32.2, so $R = I$. For Si, $F = 0.1$, $\varepsilon = 3.8$ eV, and the Mn $K_\alpha$ line occurs at 5.9 keV, which gives $R = 111$ eV. So it seems that there is not much more room for improvement. The resolution of XEDS detectors won't approach that of crystal spectrometers, which is 5 to 10 eV, although, because of the dependence of $I$ on the X-ray energy, light-element K lines have widths <<100 eV.

## 32.7. WHAT YOU SHOULD KNOW ABOUT YOUR XEDS

There are several fundamental parameters of both Si(Li) and IG XEDS systems which you can specify, measure, and monitor to ensure that your system is performing acceptably. Many of these tests are standard procedures (e.g., see the XEDS laboratories in Lyman *et al.* 1990) and have been summarized by Zemyan and Williams (1995). In an SEM, which is relatively well behaved, Si(Li) detectors have been known to last ten years or more before requiring service or replacement. In contrast, an AEM (particularly the higher-voltage variety) is a hostile environment and the life of a detector is often less than three years. For this reason, most detectors are equipped with protective shutters (see Section 33.3).

It is particularly important to monitor the detector performance on your AEM, in order that quantitative analyses you make at very different times may be compared in a valid manner.

You need to know both the operating specifications for your own system and how to measure them. We can break these specifications down into detector variables and signal-processing variables.

### 32.7.A. Detector Variables

*The detector resolution* that we just defined may degrade for a variety of reasons. Two are particularly common:

- Damage to the intrinsic region by high-energy fluxes of radiation.
- Bubbling in the liquid-$N_2$ dewar due to ice crystals building up.

You can help to minimize the ice build-up by filtering the liquid $N_2$ before putting it into the dewar. Never re-cycle liquid $N_2$ into the dewar; use it elsewhere. If the nitrogen in the dewar is bubbling, you should consider warming up the detector, but do it *after consultation with the manufacturer, and without the applied bias*. (Think what happens to the Li otherwise.) Emptying out the dewar, filling it with hot water, and then drying it with a hair dryer will often solve the problem. However, after several such cycles, you may find that the detector resolution doesn't return to acceptable levels (the window seal may develop a leak due to the repeated thermal oscillations). When this happens, it is necessary to return the detector to the manufacturer to have it repaired.

*Incomplete Charge Collection (ICC).* Because of the inevitable presence of the dead layer, the X-ray peak will not be represented by a perfect Gaussian shape when displayed after processing. Usually, the peak will have a low-energy tail, because some energy will be deposited in the dead layer and will not create detectable electron–hole pairs. You can measure this ICC effect from the ratio of the full width at tenth maximum (FWTM) to the FWHM of the displayed peak, as shown schematically in Figure 32.9.

The ideal value for FWTM/FWHM is 1.82 (Mn $K_\alpha$ or Cr $K_\alpha$), but this value will be larger for X-ray peaks from the lighter elements, which are more strongly absorbed by the detector.

In Si(Li) detectors, the phosphorus $K_\alpha$ peak shows the worst ICC effects because this X-ray fluoresces Si very efficiently. ICC will also occur if a detector has a large number of recombination sites arising, for example, through damage from a high flux of backscattered electrons. The crystal defects that act as recombination sites may be annealed out by warming the detector, as we just described. IG detectors used to show worse ICC effects than Si(Li) detectors, but this is no longer the case. Now, an IG detector should meet the same FWTM/FWHM ratio criterion as a Si(Li) detector. If the ratio is higher than 2 for the Cr peak, there is something seriously wrong with the detector and you should have it replaced.

*Detector Contamination.* Over a period of time, ice and/or hydrocarbons will eventually build up on the cold detector surface or on the window. If ice or hydrocarbon contamination does occur, it will reduce the efficiency with which we detect low-energy X-rays. While this is most

likely to happen for a windowless detector, Be and UTW systems also suffer the same problem because of residual water vapor in the detector vacuum or because the window may be slightly porous. In all cases the problem is insidious, because the effects may develop over many months and you will not notice the degradation of the spectrum until differences in light-element quantification are apparent from the same specimen analyzed at different times. Therefore, you should regularly monitor the quality of the low-energy spectrum. The ratio of the $NiK_\alpha/NiL_\alpha$ has been used (Michael 1995), but you can also use the $CrK_\alpha/CrL_\alpha$ intensity ratio on the same evaporated film of pure Cr used for resolution, as long as there is no significant oxide film, since the O $K_\alpha$ line overlaps the Cr $L_\alpha$ line.

The $NiK_\alpha/NiL_\alpha$ ratio will rise with time if contamination or ice is building up on the detector and selectively absorbing the lower-energy L line.

The K/L ratio will differ for different detector dead layers, for different UTWs or ATWs, and for different specimen thicknesses. So we can't define an accepted figure of merit. The best you can do is to measure the ratio immediately after installing a new (or repaired) detector and be aware that as the ratio increases, then any quantification involving similar low-energy X-ray lines will become increasingly unreliable. When the ratio increases to what you deem to be an unacceptably high value, then you must remove the ice/contamination. Automatic *in situ* heating devices which raise the detector temperature sufficiently to sublime the ice make this process routine. If your detector doesn't have such a device, then you should warm up the detector, as we described above.

In summary, you should measure and continually monitor changes in:

- *Your detector resolution* at the Mn or $CrK_\alpha$ line [typically 140–150 eV for Si(Li) and 120–130 eV for IG].
- *The ICC* defined by the FWTM/FWHM ratio of the Cr $K_\alpha$ line (ideally 1.82).
- *The ice build-up* reflected in the Ni (or Cr) $K_\alpha/L_\alpha$ ratio.

If any of these figures of merit get significantly larger than the accepted values, then you should have your detector serviced by the manufacturer. Warming up the detector may cure some or all of the detector problems, but it could be an expensive procedure if you get it wrong. So only do it with the bias off and after consultation with the manufacturer.

So, you must be very careful with your XEDS:

- *Do not* generate high fluxes of X-rays or backscattered electrons unless your detector is shuttered.
- *Do not* warm up the detector with the bias applied and without consulting the manufacturer.
- *Do not* use unfiltered or re-cycled liquid $N_2$.

## 32.7.B. Processing Variables

Other ways to monitor the performance of the XEDS system relate to the processing of the detector output signal. There are three things you have to check to make sure the pulse processing electronics are working properly:

- First, check the calibration of the energy range of the spectrum.
- Second, check the dead-time correction circuitry.
- Third, check the maximum output count rate.

The energy calibration should not change significantly from day to day, unless you change the range or the time constant. Electronic circuit stability has improved to a level where these three checks need only be done a few times a year (or if the detector has been repaired or a new detector installed).

*Calibration of the energy display range.* This process is quite simple; collect a spectrum from a material which generates a pair of K X-ray lines separated by about the width of the display range (e.g., Al-Cu for 0–10 keV). Some systems use an internal electronic strobe to define zero, and in this case you only need a specimen with one K line at high energy. Having gathered a spectrum, see if the computer markers are correctly positioned at the peak centroid (e.g., Al $K_\alpha$ at 1.54 keV and Cu $K_\alpha$ at 8.04 keV). If the peak and marker are more than 1 channel (10 eV) apart, then you should re-calibrate your display using the software routine supplied by the manufacturer.

*Checking the dead-time correction circuit.* If the dead-time correction circuitry is working properly, the pulse processor will give a linear increase in output counts as the input counts increase, for a fixed live time.

- Choose a specimen of a pure element, say our favorite Cr foil, which we know will give a strong $K_\alpha$ peak.
- Choose a live time, say 50 s, and a beam current to give a dead-time readout of about 10%.

- Measure the total Cr $K_\alpha$ counts that accumulate in 50 s.
- Then repeat the experiment with higher input count rates.

To increase the count rate, increase the beam current by choosing a larger-diameter beam or larger C2 aperture. The dead time should increase as the input count rate goes up, but the live time will remain at the chosen value. If you plot the number of output counts against the beam current, measured with a Faraday cup, or a calibrated exposure meter reading, then it should be linear, as shown in Figure 32.10. But you will see that it will take increasingly longer clock times to attain the preset live time. If you don't have a Faraday cup, you can use the input count rate as a measure of the current; remember that the Faraday cup is useful for many other functions, such as characterizing the performance of the electron source, as we saw in Chapter 5.

*Determination of the maximum output count rate.* Again the procedure is simple:

- Gather a spectrum for a fixed clock time, say 10 s, with a given dead time, say 10%.
- Increase the dead time by increasing the beam current, C2 aperture size, or specimen thickness.
- See how many counts accumulate in the Cr $K_\alpha$ peak.

The number of counts should rise to a maximum and then drop off, because beyond a certain dead time, which depends on the system electronics, the detector will be closed more than it is open and so the counts in a given clock time will decrease. In Figure 32.11, this maximum is at about 60%, typical of modern systems, although in older XEDS units this peak can occur at as little as 30% dead time. You

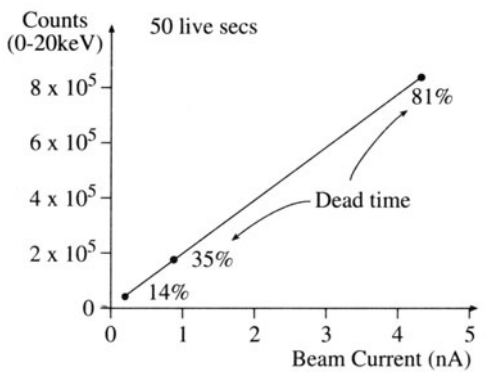


**Figure 32.10.** A plot of the output counts in a fixed live time as a function of increasing beam current showing good linear behavior over a range of dead times, implying that the dead-time correction circuitry is operating correctly.

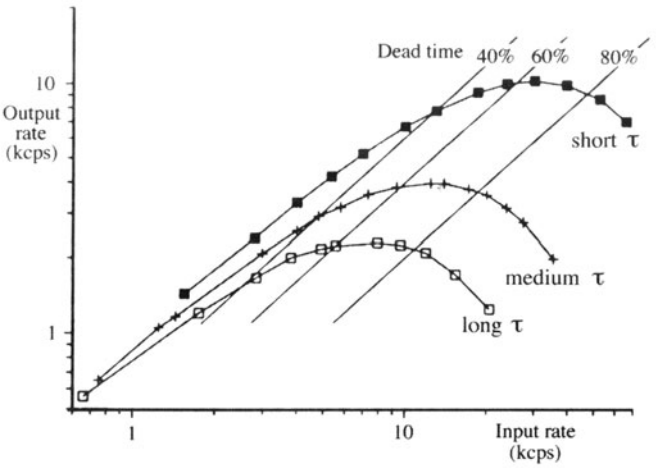


**Figure 32.11.** The output count rate in a given clock time as a function of dead time. The maximum processing efficiency is reached at about 60% dead time. It is very inefficient to use the system above the maximum output rate. Increasing the time constant results in fewer counts being processed and a drop in the output count rate.

can repeat this experiment for different time constants, $\tau$, and the counts should increase as $\tau$ is lowered (at the expense of energy resolution), as also shown in Figure 32.11. Clearly, if you operate at the maximum in such a curve (if you can generate enough input counts) then you will be getting the maximum possible information from your specimen. As we've already said, it is generally better to have more counts than to have the best energy resolution, so select the shortest $\tau$ unless you have a peak overlap problem.

While it is rare that a good thin foil produces enough X-ray counts to overload modern detector electronics, there are situations (e.g., maximizing analytical sensitivity) when it's desirable to generate as many counts as possible. Under these circumstances, use of thicker specimens and high beam currents may produce too many counts for conventional analog processing systems. As shown in Figure 32.12A, digital processing permits a higher throughput over a continuous range of energy resolution than the fixed ranges available from specific (in this case, six) time constants. Even more dramatic, as shown in Figure 32.12B, megahertz-rate beam blanking, which deflects the beam off the specimen as soon as the XEDS detects an incoming pulse, permits a remarkable increase in throughput (Lyman *et al.* 1994).

If your specimen is too thin, it might not be possible to generate sufficient X-ray counts to reach dead times in excess of 50%, so the curve may not reach a maximum, particularly if $\tau$ is very short. In this case, just use a thicker specimen.

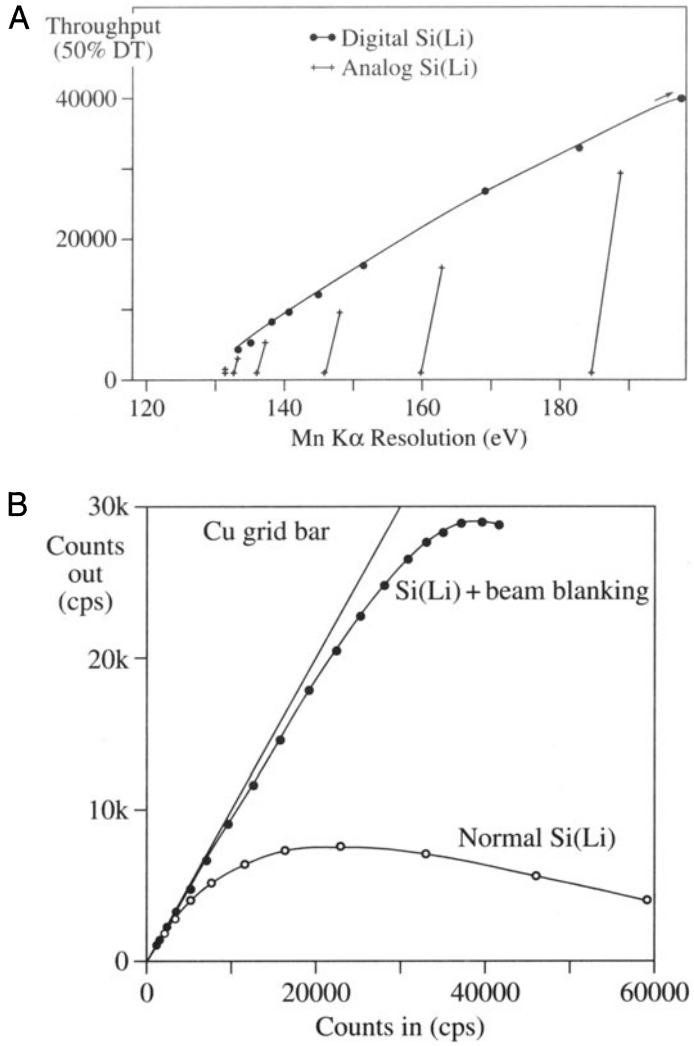


**Figure 32.12.** (A) Digital pulse processing gives a continuous range of X-ray throughput at 50% dead time, compared with a set of fixed throughput ranges for specific analog processing time constants. (B) Megahertz beam blanking results in a four times improvement in X-ray throughput compared to processing without beam blanking.

In summary you should occasionally:

- Check the energy calibration of the MCA display.
- Check the dead-time circuitry by the linearity of the output count rate versus beam current.
- Check the counts in a fixed clock time as a function of beam current to determine the maximum output count rate.

## 32.7.C. Artifacts Common to XEDS Systems

The XEDS system introduces its own artifacts into the spectrum. Fortunately, we understand all these artifacts, but they still occasionally mislead the unwary operator; see the review by Newbury (1995). We can separate the artifacts into two groups:

- Signal-detection artifacts. Examples are "escape" peaks and "internal fluorescence" peaks.
- Signal-processing artifacts. One example is "sum" peaks.

*Escape peak.* Because the detector is not a perfect "sink" for all the X-ray energy, it is possible that a small fraction of the energy is lost and not transformed into electron–hole pairs. The easiest way for this to happen is if the incoming photon of energy $E$ fluoresces a Si $K_\alpha$ X-ray (energy 1.74 keV) which escapes from the intrinsic region of the detector. The detector then registers an energy of ($E$-1.74) keV. An example is shown in Figure 32.13.

Si "escape peaks" appear in the spectrum 1.74 keV below the true characteristic peak position.

The magnitude of the escape peak depends on the design of the detector and the energy of the fluorescing X-ray. The most efficient X-ray to fluoresce Si $K_\alpha$ X-rays is the P $K_\alpha$, but in a well-designed detector even the P escape peak will only amount to < 2% of the P $K_\alpha$ intensity. This fact explains why you can only see escape peaks if there are major characteristic peaks in the spectrum. More escape peaks occur in IG spectra because we can fluoresce both Ge $K_\alpha$ (9.89 keV) and $L_\alpha$ (1.19 keV) characteristic X-rays in the detector. Each of these can cause corresponding escape peaks, but the $L_\alpha$ has much less chance of escaping.

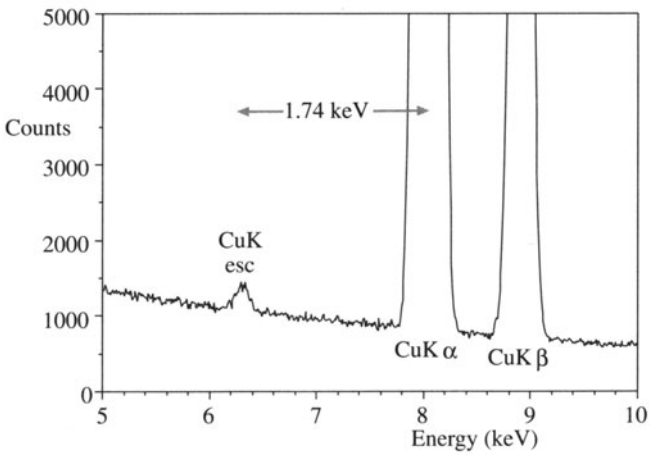


**Figure 32.13.** The escape peak in a spectrum from pure Cu, 1.74 keV below the Cu $K_\alpha$ peak. The intense $K_\alpha$ peak is truncated because it is ~50–100 times more intense than the escape peak.

The quantitative analysis software should be able to recognize any escape peak in the spectrum, remove it, and add the intensity back into the characteristic peak where it belongs. Because the escape peak intensity is so small it is rarely a problem.

*The internal-fluorescence peak.* This is a characteristic peak from the Si or Ge in the detector dead layer. Incoming photons can fluoresce atoms in the dead layer and the resulting Si $K_\alpha$ or Ge K/L X-rays enter the intrinsic region of the detector, which cannot distinguish their source and therefore registers a small peak in the spectrum. As detector design has improved and dead layers have decreased in thickness, the internal-fluorescence peak artifact has shrunk. However, it has not yet disappeared entirely.

A small Si $K_\alpha$ peak will occur in all spectra from Si(Li) detectors for long counting times.

Obviously you must be wary when looking for small amounts of Si in a specimen, because you'll always find it! Depending on the detector, particularly the dead-layer thickness, the Si signal has an intensity corresponding to about 0.1% to 1% of the composition of the specimen (see Figure 32.14), so again it is not a major problem. Similar effects are observed in IG detectors also. The Au absorption edge from the ohmic contact layer at the front end of the detector is sometimes detectable as a small disturbance in the bremsstrahlung intensity, around 1 keV, but the effect on microanalysis is negligible.

*Sum peak.* As we described earlier, the processing electronics are designed to switch off the detector while each pulse is analyzed and assigned to the correct energy channel. The sum peak arises when the electronics are not fast enough. We can identify the conditions where this is likely to occur:

- The input count rate is high.
- The dead times are in excess of about 60%.
- There are major characteristic peaks in the spectrum.

The system simply cannot be perfect. Occasionally two photons will enter the detector at almost exactly the same time. The analyzer then registers an energy corresponding to the sum of the two photons. Since this event is most likely for the X-ray giving the major peak, a sum peak (sometimes called a coincidence or double peak) appears at twice the energy of the major peak, as shown in Figure 32.15.

The sum peak should be invisible if you maintain a reasonable input count rate, typically < 10,000 cps, which should give a dead time of < 60%.

In an AEM, you can't usually generate such high count rates unless your specimen is very thick. As always, you should at least be aware of the danger. For example, the Ar $K_\alpha$ energy is almost exactly twice the Al $K_\alpha$ energy. In the past the sum peak has led some researchers to report argon being present in aluminum specimens when it wasn't, and others to ignore argon which actually was present in ion-milled specimens! As detector electronics have improved, the sum peak has ceased to cause significant problems, except for intense low-energy peaks below ~1.25 keV, e.g., Mg $K_\alpha$, where the residual noise in the electronic circuitry interferes with the pile-up rejection. So

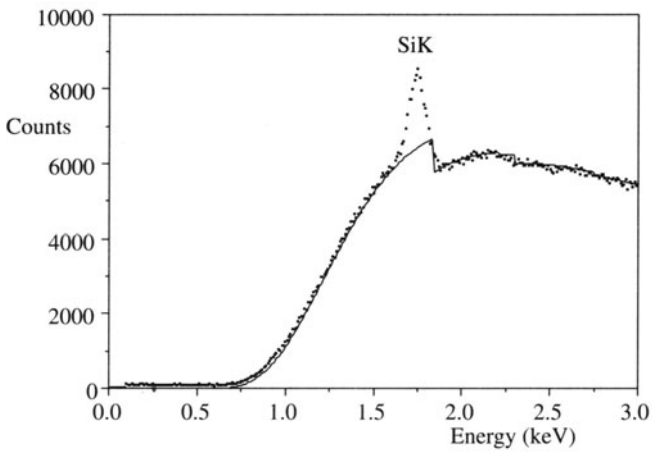


**Figure 32.14.** The Si internal fluorescence peak in a spectrum from pure C obtained with a Si(Li) detector. The ideal spectrum is fitted as a continuous line which exhibits the Si K absorption edge only.

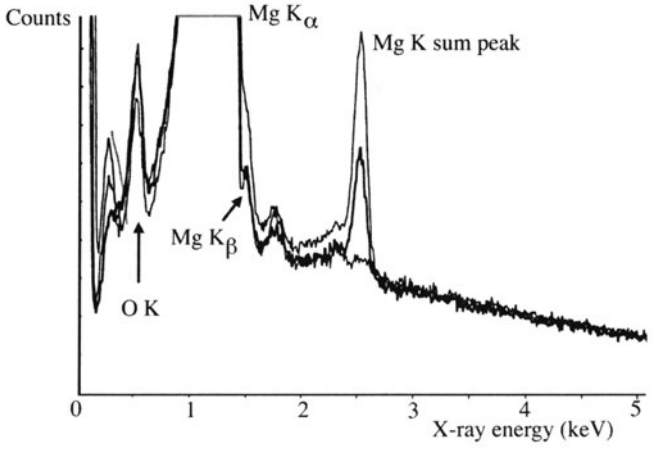


**Figure 32.15.** The Mg sum (coincidence) peak at various dead times; upper trace 70% dead time, middle trace 47%, lower trace 14%. The artifact is absent at 14% dead time.

if you're analyzing lighter elements than Mg, take care to use low input count rates. Reducing the dead time to 10–20% should remove even the Mg $K_\alpha$ sum peak, as shown in Figure 32.15.

Much of what we have just discussed can be observed experimentally on the AEM. But it is often just as instructive, and certainly easier, to simulate the spectra. To this end, we strongly advise you to purchase the simulation software Desktop Spectrum Analyzer (DTSA) from NIST, which is listed in the recommended software in Section 1.5. This software permits realistic simulation of XEDS spectra in TEMs (and SEMs) and introduces you to all the aspects of spectral processing, artifacts, modeling, etc., that are discussed in the next four chapters.

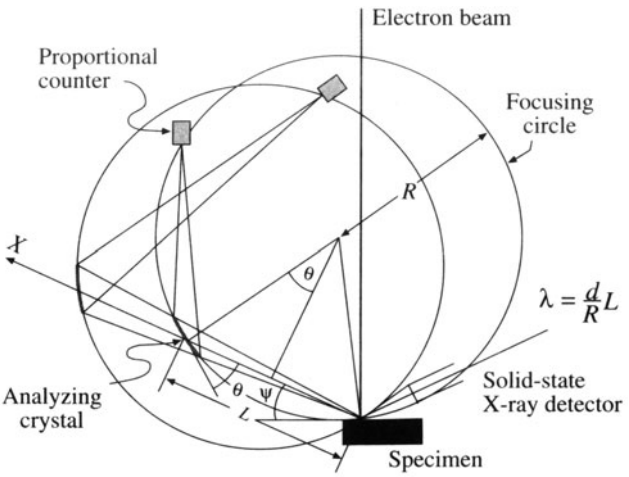


**Figure 32.16.** Schematic diagram of a WDS system showing how the specimen, crystal, and detector are constrained to move on the focusing circle, radius *R*, such that the specimen–crystal distance *L* is directly proportional to the X-ray wavelength.

## 32.8. WAVELENGTH-DISPERSIVE SPECTROMETERS

Before the invention of the XEDS, the wavelength-dispersive spectrometer (WDS), or crystal spectrometer, was widely used. The WDS uses one or more diffracting crystals of known interplanar spacing, as devised by W. H. Bragg in 1913. Bragg's Law ($n\lambda = 2d\sin\theta$), which we've already come across in Part II, also describes the dispersion of X-rays of a given wavelength $\lambda$ through different scattering angles, $2\theta$. We accomplish this dispersion by placing a single crystal of known interplanar spacing ($d$) at the center of a focusing circle which has the X-ray source (the specimen) and the X-ray detector on the circumference, as shown in Figure 32.16. The detector is usually a gas-flow proportional counter, but there's no reason why it couldn't be a Si(Li) or Ge semiconductor detector. In fact, these detectors may see more use as the need for better vacuums increases.

The mechanical motions of the crystal and detector are coupled such that the detector always makes an angle $\theta$ with the crystal surface while it moves an angular amount $2\theta$ as the crystal rotates through $\theta$. By scanning the spectrometer, a limited range of X-ray wavelengths of about the same dimension as the $d$-value of the analyzing crystal can be detected. For example, diffraction from the (200) planes of a LiF crystal covers an energy range of 3.5–12.5 keV (0.35–0.1 nm) for a scanning range of $\theta$ = 15–65°. To detect X-rays outside this energy range, another crystal of different $d$-value must be employed.

As we'll discuss in Chapter 35, the forerunner of the AEM was the electron microscope microanalyzer (EMMA), which used a WDS. However, the WDS was a large and inefficient addition to the microscope, and never attained general acceptance by transmission microscopists.

There are two major drawbacks to the WDS compared with the XEDS:

- The crystal has to be moved to a precise angle where it collects only a tiny fraction of the total number of X-rays coming from the specimen, whereas the XEDS detector can be placed almost anywhere in the TEM stage above the specimen and subtends a relatively large solid angle at the specimen.
- The WDS collects a single wavelength at a given time while the XEDS detects X-rays of a large range of energies. WDS is a serial collector; XEDS is effectively a parallel collector.

The geometrical advantage in the collection efficiency of XEDS, combined with the ability to detect X-rays simultaneously over a wide energy range without the mechanical motion required of the WDS, accounts for the present dominance of XEDS systems in all types of electron microscopes. However, there are several advantages of WDS over XEDS:

- Better energy resolution (5–10 eV) to unravel the peak overlaps that plague XEDS (see Section 34.3).
- Better peak-to-background capability to detect smaller amounts of elements.
- Better detection of light elements (minimum $Z$ = 4, Be) by careful choice of crystal, rather than solely through a dependence upon electronics as in the XEDS.

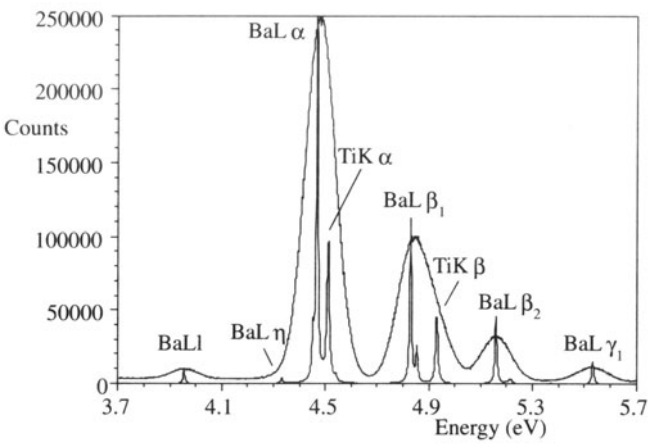


**Figure 32.17.** A WDS spectrum from $BaTiO_3$, but plotted against energy rather than wavelength. WDS easily resolves the Ba $L_\alpha$/Ti $K_\alpha$ overlap, which is impossible with an EDS as shown in the overlapping spectrum. The improved resolution of WDS (~8 eV) is obvious.

- No artifacts in the spectrum from the detection and signal processing, except for higher-order lines from fundamental reflections (when $n \geq 2$ in the Bragg equation).
- Higher throughput count rate using a gas-flow proportional counter.

A typical WDS spectrum from $BaTiO_3$ is shown in Figure 32.17. For comparison, an XEDS spectrum is shown superimposed; the improved resolution and *P/B* for WDS are obvious. Because of these advantages, the WDS is often the spectrometer of choice in the X-ray fluorescence spectrometer (XRF), which has a spatial resolution of a few millimeters, and in the electron probe microanalyzer (EPMA) with a spatial resolution of a few micrometers. The advantages of the WDS may make it an attractive complement to the XEDS in future AEMs. However, WDS systems have not been applied to AEMs because of their low X-ray collection efficiency compared to the XEDS, and we discussed the drawbacks of WDS at the start of the chapter. Only when a WDS is designed that is compact enough to be placed inside an AEM specimen stage will it be possible to realize these advantages, and even then the output count rate from thin specimens might be too low unless the AEM has an FEG (Goldstein *et al.* 1989). Spence and Lund (1991) show preliminary results from a WDS in an AEM giving 40-eV resolution in a study of coherent bremsstrahlung (see Section 33.4.C).

## CHAPTER SUMMARY

The XEDS is the only X-ray spectrometer currently used in TEMs. It is remarkably compact, efficient, and sensitive. A combination of Si(Li) and Ge detectors can detect $K_\alpha$ lines from all the elements, from Be to U. However, the XEDS has limits in terms of its need for cooling, its poor energy resolution, and the many artifacts that appear in the spectra. The XEDS is simple to run and maintain if you take care to perform certain basic procedures and refrain from certain others that can damage the detector. Sometimes, it may be too simple; beware. You need to:

- Measure your detector resolution weekly at the Mn or Cr $K_\alpha$ line (typically, 130–140 eV for Si(Li) and 120–130 eV for IG).
- Measure the ICC defined by the FWTM/FWHM ratio of the Cr $K_\alpha$ line (ideally 1.82) on a monthly basis.
- Monitor any ice build-up via the Ni (or Cr) $K_\alpha/L_\alpha$ ratio on a weekly basis.
- Check the calibration of the energy range of your MCA display every few months.
- Check the dead-time correction circuitry by the linearity of the output count rate versus beam current, every six months.
- Check the counts in a fixed clock time as a function of beam current, to determine the maximum output count rate, every six months.
- Be aware of artifacts in *all* your spectra.

For the sake of completeness, Table 32.1 below shows you the relative merits of the various detectors that we have discussed in this chapter.

**Table 32.1. Comparison of X-ray Spectrometers**

| Characteristic energy resolution | Intrinsic Ge | Lithium-drifted Si | WDS |
|---|---|---|---|
| Typical value | 140 eV | 150 eV | 10 eV |
| Best value | 114 eV | 127 eV | 5 eV |
| Energy required to form electron–hole pairs (77 K) | 2.9 eV | 3.8 eV | n.a. |
| Band-gap energy (indirect) | 0.67 eV | 1.1 eV | n.a. |
| Cooling required | $LN_2$ or thermoelectric | $LN_2$ or thermoelectric | none |
| Typical detector active area | 10–30 $mm^2$ | 10–30 $mm^2$ | n.a. |
| Typical output counting rates | 5–10,000 cps | 5–10,000 cps | 50,000 cps |
| Time to collect full spectrum | 1 min | 1 min | 30 min |
| Collection angle | 0.03–0.20 sr | 0.03–0.30 sr | $10^{-4}$–$10^{-3}$ sr |
| Take-off angle | 0°/20°/72° | 0°/20°/72° | 40°–60° |
| Artifacts | Escape peaks<br>Sum peaks<br>Ge K/L internal fluorescence peaks | Escape peaks<br>Sum peaks<br>Si K internal fluorescence peaks | High-order lines |

# REFERENCES

## General References


Goldstein, J.I., Newbury, D.E., Echlin, P., Joy, D.C., Romig, A.D. Jr., Lyman, C.E., Fiori, C.E., and Lifshin, E. (1992) *Scanning Electron Microscopy and X-ray Microanalysis,* 2nd edition, Plenum Press, New York.

Heinrich, K.F.J., Newbury, D.E., Myklebust, R.L., and Fiori, C.E., Eds. (1981) *Energy Dispersive X-ray Spectrometry,* NBS Special Publication 604, U.S. Department of Commerce, Washington, DC.

Russ, J.C. (1984) *Fundamentals of Energy Dispersive X-ray Analysis,* Butterworths, Boston, Massachusetts.

Williams, D.B., Goldstein, J.I., and Newbury, D.E., Eds. (1995) *X-Ray Spectrometry in Electron Beam Instruments,* Plenum Press, New York.


## Specific References


Goldstein, J.I., Lyman, C.E., and Williams, D.B. (1989) *Ultramicroscopy* **28**, 162.

Joy, D.C. (1995) in *X-Ray Spectrometry in Electron Beam Instruments* (Eds. D.B. Williams, J.I. Goldstein, and D.E. Newbury), p. 53, Plenum Press, New York.

Lund, M.W. (1995) *ibid.,* p. 21.

Lyman, C.E., Newbury, D.E., Goldstein, J.I., Williams, D.B., Romig, A.D. Jr., Armstrong, J.T., Echlin, P.E., Fiori, C.E., Joy, D.C., Lifshin, E., and Peters, K.R. (1990) *Scanning Electron Microscopy, X-Ray Microanalysis and Analytical Electron Microscopy; A Laboratory Workbook,* Plenum Press, New York.

Lyman, C.E., Goldstein, J.I., Williams, D.B., Ackland, D.W., von Harrach, S., Nicholls, A.W., and Statham, P.J. (1994) *J. Microsc.* **176**, 85.

McCarthy, J.J. (1995) in *X-Ray Spectrometry in Electron Beam Instruments* (Eds. D.B. Williams, J.I. Goldstein, and D.E. Newbury) p. 67, Plenum Press, New York.

Michael, J.R. (1995) *ibid.,* p. 83.

Mott, R.B. and Friel, J.J. (1995) *ibid.,* p. 127.

Newbury, D.E. (1995) *ibid.,* p. 167.

Sareen, R.A. (1995) *ibid.,* p. 33.

Spence, J.C.H. and Lund, M. (1991) *Phys. Rev.* **B44**, 7054.

Statham, P.J. (1995) in *X-Ray Spectrometry in Electron Beam Instruments* (Eds. D.B. Williams, J.I. Goldstein, and D.E. Newbury), p. 101, Plenum Press, New York.

Zemyan, S.M. and Williams, D.B. (1994) *J. Microsc.* **174**, 1.

Zemyan, S.M. and Williams, D.B. (1995) *X-Ray Spectrometry in Electron Beam Instruments* (Eds. D.B. Williams, J.I. Goldstein, and D.E. Newbury), p. 203, Plenum Press, New York.